

On the Dimers of Pseudoisocyanine

P.O.J. Scherer*

Physics Department T38, TU Munich, 85748 Garching

Abstract

The self organisation of pseudoisocyanine-dimers in dilute aqueous solutions is studied by classical MD simulations. The electronic structure of the dimer is evaluated with the semiempirical ZINDO method to determine the fluctuations of site energies and excitonic coupling. We study different dimer conformations with blue or red shifted absorption maxima as models for H and J-aggregates. The width of the absorption bands is mainly explained by low frequency vibrations whereas the fluctuations of site energies are less important.

I. INTRODUCTION

Since the discovery of the so called J-band^{1,2}, an unusual sharp absorption band which is characteristic for the aggregation of the classical sensitizing dye 1,1'-diethyl-2,2'-cyaninchloride (pseudisocyanine) a large amount of experimental and theoretical work addressed the investigation of molecular aggregates and their red shifted J-bands. At lower concentration blue shifted H-bands were observed which were attributed to molecular dimers, the smallest possible aggregates. Molecular modelling of the J-aggregates is difficult due to the fact that the PIC molecule is a cation and therefore the Coulombic interactions as well as dielectric shielding have to be taken into account carefully. For the formation of larger aggregates the counterions are important whereas this seems not the case for the smaller H-aggregates³. Therefore we started the simulation of PIC aggregates by a detailed investigation of the dimer. From the analysis of the experimental spectrum in water⁴ it was deduced that both excitonic components contribute with an intensity ratio of 2:1. This can not be explained⁵ by dimer models^{4,6} where the dipole moments are almost parallel or antiparallel as it is the case for the common brickwork or ladder models which are found in the literature for the J-aggregate^{7,8}. Another focus of our investigations concerns the contribution of local Coulombic interactions to the inhomogeneous broadening of the site energies and its importance in comparison to intramolecular vibrations.

II. METHODS

For the classical MD simulation we used the model of rigid rotors which can be easily combined with quantum calculations to obtain electronic excitations and coupling matrix elements⁹. Since also the position of the ethyl groups is fixed we have to distinguish not only two stereoisomers but also a fully C₂-symmetric form and another form where the ethyl-groups break this symmetry. A possible interconversion between these conformations was not taken into account.

We simulated a cube containing a pair of PIC (positively charged) molecules and 2150 TIP5¹⁰ water molecules. We did not use periodic boundary conditions to avoid artefacts from the Coulombic interaction with the mirror images. Instead reflecting boundaries kept the molecules from escaping the box by reversing the normal velocity component whenever the

center of mass of one of the molecules encountered the boundary . The boundary distance of 36Å was adjusted to reproduce the experimental density of water at room temperature. The equations of motion were solved using an implicit quaternion method¹¹ for the rotations and a Leap frog method for the translations. The timestep used was 1 fsec.

In our simulation we neglected electrostatic interactions with solvent outside the cube. We calculated the missing contribution to the solvation energy from a simple PCM model¹². The simulated box was put into a cubic cavity in a dielectric continuum and the contribution to the solvation energy was calculated from the interaction between the charges within the box and the induced surface charges. It gave 13% of the total solvation energy. This value stayed rather constant along the trajectory. Therefore we assume that the essential changes of interaction with solvent molecules in the immediate surroundings are taken into account sufficiently.

The force field was designed to reproduce the local electrostatic interactions properly, which is especially important for the large sized PIC molecule with its extended π -electron system. It is based on a simplified version of the effective fragment model¹³⁻¹⁵. The charge distribution is approximated by distributed multipoles which were calculated with GAMESS on the basis of TZV/HF wavefunctions¹⁶. For the simulation only point charges q_i and dipoles \vec{p}_i were used which are centered at the positions of the nuclei and the bond centers. The Coulombic interaction energy is

$$V_{ij}^{Coul} = \frac{q_i q_j}{4\pi\epsilon_0 R_{ij}} + \frac{\vec{R}_{ij}(q_i \vec{p}_j - q_j \vec{p}_i)}{4\pi\epsilon_0 R_{ij}^3} + \frac{R_{ij}^2 \vec{p}_i \vec{p}_j - 3(\vec{R}_{ij} \vec{p}_i)(\vec{R}_{ij} \vec{p}_j)}{4\pi\epsilon_0 R_{ij}^5} \quad (1)$$

The values of point charges and dipoles are given for the symmetry unique atoms in Table I.

The electronic spectra were calculated on the ZINDO/CI-S level¹⁷ including the point monopoles and dipoles of all water molecules. The two lowest excited states of the dimer are to a large extent linear combinations of the lowest monomer excitations with only very small admixture of higher monomer excitations and of charge resonance states. Therefore we use a simple 2-state model to analyze the delocalized dimer states in terms of the local excitations A^* and B^* . The interaction matrix is

$$\begin{pmatrix} \bar{E} - \Delta/2 & V \\ V & \bar{E} + \Delta/2 \end{pmatrix} \quad (2)$$

with the average monomer transition energy $\bar{E} = (E_{A^*} + E_{B^*})/2$, their splitting $\Delta = E_{B^*} - E_{A^*}$ and the excitonic coupling V . Its eigenvectors are the two delocalized dimer excitations which are written with mixing coefficients $\cos \gamma, \sin \gamma$ as

$$|1 \rangle = \cos \gamma |A^* \rangle + \sin \gamma |B^* \rangle \quad |2 \rangle = -\sin \gamma |A^* \rangle + \cos \gamma |B^* \rangle \quad (3)$$

The transition dipoles of these two states

$$\vec{\mu}_1 = \cos \gamma \vec{\mu}_{A^*} + \sin \gamma \vec{\mu}_{B^*} \quad \vec{\mu}_2 = \sin \gamma \vec{\mu}_{A^*} - \cos \gamma \vec{\mu}_{B^*} \quad (4)$$

are linear combinations of the transition dipoles $\vec{\mu}_{A^*,B^*}$ of the two monomers which are assumed to be independent from the excitonic interaction. Therefore the mixing angle γ can be determined from a least square fit of the two dimer transition dipoles to (4). Then the elements of the interaction matrix are calculated from the transition energies of the two dimer excitations as

$$\bar{E} = \frac{E_1 + E_2}{2} \quad (5)$$

$$\Delta = (\cos(\gamma)^2 - \sin(\gamma)^2)(E_2 - E_1) \quad (6)$$

$$V = \cos(\gamma) \sin(\gamma)(E_2 - E_1) \quad (7)$$

We want to emphasize that this analysis is based on the delocalized dimer orbitals. It does not involve any kind of multipole expansion, especially the calculated excitonic coupling is not of the dipole-dipole type which would be quite questionable at such short intermolecular distances. To check the quality of the ZINDO method, we compared the results for a selected sandwich dimer configuration with a much more elaborate 631G** HF/CI calculation. The calculated transition dipoles of the two lowest singlet excitations were very similar (3 and 16 Debyes from ZINDO, 2 and 14 Debyes from HF/CI), the excitonic splitting was somewhat larger for the HF/CI method (0.54eV as compared to 0.37eV for ZINDO). Both methods placed the lowest charge resonance states at about 0.65 eV above the upper excitonic band.

III. RESULTS

We determined the vibronic coupling parameters for the PIC monomer as described in our earlier paper¹⁸. Application of ab initio methods¹⁶ improved the quality of the results

so that a direct comparison with the profile of the absorption spectrum becomes feasible. The normal modes were calculated on the 6-31G/MP2 level and the coupling to the optical transition on the CI/SD level. Using these couplings and the displaced harmonic oscillator model the lineshape was calculated as the Fourier transformed time correlation function. In the low frequency region the largest vibronic couplings are found for normal modes at 40 and 46 cm^{-1} which contribute significantly to the broadening of the absorption band. Another important contribution from modes around 1500 cm^{-1} which are also known from Raman spectra is the origin of the observed vibrational progression. Further modes between 50 and 1400 cm^{-1} form a rather dense continuum of coupling states. The simulated spectrum (fig. 2) largely resembles the experimental absorption profile. The width of the simulated bands is somewhat too small and the intensity of the prominent stretching modes is slightly overestimated. This could be possibly further improved by taking frequency changes and mode coupling into account.

The MD simulations were started from several plausible dimer structures. First the PIC molecules were kept fixed and the solvent was equilibrated for 50 psec. Then the restraints were removed and the system was simulated for another 50 psec. The distance and orientation of the two PIC molecules were analyzed to identify periods of relative stability.

Starting from a sandwich structure, a rather stable structure evolved within 10 psec (fig.3a). It is not symmetric but still there is almost no splitting of the calculated site energies (Table 2) which show rapid fluctuations with components down to 20fsec. Such fast fluctuations are well known from experimental and theoretical work on the dynamics of dephasing and solvation in molecular liquids¹⁹. They have been attributed to the inertial motion of the solvent molecules, which show up as the Gaussian shaped rapid initial decay of the solvation time correlation function^{20,21}. In our simulations the orientational time correlation function of the water molecules can be described by a Gaussian with a correlation time of 60 fs at short times. The time correlation of the electrostatic potential decays faster. The initial Gaussian decay with 20 fs is very similar to that of the correlation function of the transition energies. Probably collective librational motions contribute more efficiently to the electronic dephasing than the motion of the individual molecules.^{19,22}

The center of the site energies is shifted by 0.06 eV to lower energies as compared to a monomer in vacuum and the variance of the site energies is comparable to that of a monomer. The two transition dipoles are almost parallel and the lower transition carries

only 2% of the total oscillator strength. The excitonic coupling shows fluctuations similar to the site energies. Its variance, however, amounts to only 7% of the average value of 0.25eV. Hallermeier et al⁴ deduced a smaller excitonic coupling of 0.078 eV. Most probably their dimer spectrum has some admixture of the monomer spectrum. We assume that the absorption maximum at 520nm is due to monomers and the maximum of the real dimer spectrum is at 480nm. This would be consistent with an H-aggregate with an excitonic coupling of 0.2eV.

We studied also brickwork structures as a model for the J-aggregates with a red shifted absorption. We found a relative stable structure which is shown in fig. 3b. The structural fluctuations are much larger than for the sandwich model but the fluctuations of site energies and excitonic coupling are even somewhat smaller. The coupling of -0.064eV is close to the value of -0.078eV which was used to simulate the vibronic spectrum of the J-aggregates¹⁸.

Acknowledgments

This work has been supported by the Deutsche Forschungsgemeinschaft (SFB 533)

* Electronic address: philipp.scherer@ph.tum.de

- ¹ G.Scheibe, *Angew. Chemie* **49**, 563 (1936)
- ² E.E.Jelley, *Nature* **138**, 1009 (1936)
- ³ B.Neumann, *J.Phys.Chem. B* **105**, 8268 (2001)
- ⁴ B.Kopainsky, J.K.Hallermeier and W.Kaiser, *Chem.Phys.Lett.* **83**, 498 (1981)
- ⁵ G.R.Bird, K.S.Norland, A.E.Rosenoff, H.B.Michaud, *Phot.Sci.Eng.* **12**, 196 (1968)
- ⁶ R.E.Graves, P.I.Rose, *J.Phys.Chem.* **79**, 746 (1975)
- ⁷ H.J.Nolte, *Chem.Phys.Lett.* **31**, 134 (1975)
- ⁸ G.Scheibe, *Z.Elektrochemie*, **52**, 283 (1948)
- ⁹ P.O.J.Scherer, *J.Phys.Chem. A* **104**, 6301 (2000)
- ¹⁰ M.W.Mahoney, W.L.Jorgensen, *J.Chem.Phys.* **112**, 8910 (2000)
- ¹¹ I.P.Omelyan, *Phys.Rev.E* **58**, 1169 (1998)
- ¹² H.Li, C.S.Pomelli, J.H.Jensen, *Theor. Chem. Acc.* **109**, 71 (2003)

- ¹³ M.S.Gordon, M.A.Freitag, P.Bandyopadhyay, J.H.Jensen, V.Kairys, W.J.Stevens
J.Phys.Chem.A **105**, 293 (2001)
- ¹⁴ P.N.Day, J.H.Jensen, M.S.Gordon and S.P.Webb, W.J.Stevens and M.Krauss, D.Garmer,
H.Basch and D.Cohen J.Chem.Phys. **105**, 1968 (1996)
- ¹⁵ W.Chen, M.S.Gordon, J.Chem.Phys., **105**, 11081(1996)
- ¹⁶ GAMESS - M.W.Schmidt, K.K.Baldrige, J.A.Boatz, S.T.Elbert, M.S.Gordon, J.J.Jensen,
S.Koseki, N.Matsunaga, K.A.Nguyen, S.Su, T.L.Windus, M.Dupuis, J.A.Montgomery
J.Comput.Chem. **14**, 1347 (1993)
- ¹⁷ M.A.Thompson. M.C.Zerner, J.Am Chem.Soc. **112**, 7828 (1990)
- ¹⁸ P.O.J.scherer, in: J-Aggregates, ed. T.Kobayashi, World scientific, p.95 (1996)
- ¹⁹ E.T.J.Nibbering, D.A.Wiersma, K.Duppen, Chem.Phys. **183**, 167 (1994)
- ²⁰ M.Maroncelli, J.Chem.Phys. **94**, 2084 (1991)
- ²¹ E.A.Carter, J.T.Hynes, J.Chem.Phys. **94**, 5961 (1991)
- ²² T.Hayashi, T. la Cour Jansen, Wei Zhuang, and S.Mukamel, J.Phys.Chem. A **109**, 64 (2005)

IV. TABLE CAPTIONS

Table I:

coordinates, atomic charges and dipoles for PIC

Table II:

mean values and standard deviation of distances, orientation angles, excitation energies and excitonic couplings for the two structures. The long axis is defined by the vector connecting the two nitrogen atoms $\mathbf{R}(N_{13}) - \mathbf{R}(N_{14})$, the short axis by the vector $\mathbf{R}(N_{14}) - \mathbf{R}(C_{20}) + \mathbf{R}(N_{13}) - \mathbf{R}(C_{19})$.

Table I:

label	x(Bohr)	y(Bohr)	z(Bohr)	q	$p_x(e \bullet Bohr)$	$p_y(e \bullet Bohr)$	$p_z(e \bullet Bohr)$
C 1	-9.565	1.113	-3.478	0.973	0.000	0.044	0.092
C 3	-7.152	0.889	-2.403	0.929	0.038	-0.017	0.029
C 5	-6.682	1.814	0.029	0.928	0.046	0.017	0.005
C 7	-8.685	2.931	1.361	0.857	-0.014	-0.025	-0.090
C 9	-11.028	3.132	0.263	1.055	0.105	-0.062	-0.039
C11	-11.494	2.232	-2.174	0.992	0.101	-0.009	0.026
N13	-4.247	1.613	1.055	0.472	-0.038	-0.096	-0.101
C15	-2.340	0.409	-0.158	0.997	-0.061	0.124	0.024
C17	-2.850	-0.583	-2.637	0.738	-0.052	0.121	0.041
C19	-5.129	-0.334	-3.709	1.046	0.019	0.001	0.116
C21	-3.738	2.886	3.487	0.859	-0.053	-0.089	-0.108
C23	-4.351	1.265	5.791	0.893	0.020	-0.005	-0.027
C25	0.000	0.000	1.050	0.421	0.000	0.000	-0.310
H27	-1.393	-1.638	-3.559	0.393	0.072	0.038	0.027
H29	-5.484	-1.128	-5.546	0.341	0.003	-0.020	-0.040
H31	-8.451	3.626	3.244	0.331	-0.016	0.024	0.046
H33	-12.532	3.997	1.319	0.347	-0.033	0.016	0.015
H35	-13.340	2.406	-2.997	0.351	-0.036	0.003	-0.016
H37	-9.869	0.384	-5.351	0.331	-0.028	-0.008	-0.037
H39	-1.778	3.440	3.479	0.319	0.024	0.010	-0.006
H41	-4.812	4.618	3.507	0.313	-0.023	0.024	-0.001
H43	-6.323	0.721	5.833	0.299	-0.033	-0.015	0.012
H45	-3.944	2.325	7.497	0.315	0.002	0.013	0.035
H47	-3.236	-0.453	5.827	0.271	0.003	-0.036	0.020

label	x(Bohr)	y(Bohr)	z(Bohr)	q	$p_x(e \bullet Bohr)$	$p_y(Bohr)$	$p_z(e \bullet Bohr)$
BO31	-8.358	1.001	-2.940	-0.591	-0.156	0.084	0.045
BO53	-6.917	1.351	-1.187	-0.737	-0.091	0.047	-0.017
BO75	-7.683	2.372	0.695	-0.642	-0.075	-0.008	0.003
BO97	-9.856	3.032	0.812	-0.820	-0.051	0.026	-0.020
BO111	-10.529	1.672	-2.826	-0.889	-0.029	0.021	0.054
BO119	-11.261	2.682	-0.956	-0.693	0.049	-0.074	-0.055
BO135	-5.464	1.713	0.542	-0.348	-0.128	0.109	-0.133
BO1513	-3.293	1.011	0.449	-0.450	0.093	-0.118	-0.042
BO1715	-2.595	-0.087	-1.398	-0.495	0.080	-0.050	-0.035
BO193	-6.140	0.277	-3.056	-0.488	-0.014	-0.194	0.034
BO1917	-3.989	-0.459	-3.173	-0.905	0.001	-0.013	0.010
BO2113	-3.993	2.250	2.271	-0.125	0.086	0.192	0.103
BO2321	-4.045	2.076	4.639	-0.341	-0.016	-0.003	0.074
BO2515	-1.170	0.204	0.446	-0.609	-0.082	-0.320	0.223
BO2625	0.000	0.000	2.056	-0.447	0.000	0.000	-0.209
BO2717	-2.121	-1.111	-3.098	-0.506	-0.137	0.205	0.099
BO2919	-5.306	-0.731	-4.627	-0.525	0.037	0.121	0.276
BO317	-8.568	3.279	2.303	-0.537	-0.046	-0.114	-0.263
BO339	-11.780	3.565	0.791	-0.547	0.237	-0.131	-0.159
BO3511	-12.417	2.319	-2.586	-0.551	0.285	-0.028	0.126
BO371	-9.717	0.748	-4.415	-0.538	0.061	0.109	0.278
BO3921	-2.758	3.163	3.483	-0.555	-0.314	-0.072	0.041
BO4121	-4.275	3.752	3.497	-0.529	0.200	-0.282	0.023
BO4323	-5.337	0.993	5.812	-0.543	0.350	0.089	-0.009
BO4523	-4.148	1.795	6.644	-0.510	-0.074	-0.199	-0.303
BO4723	-3.794	0.406	5.809	-0.518	-0.218	0.302	-0.004

Table II:

	sandwich	brickwork
excitation energy E_a	$2.522 \pm 0.014 eV$	$2.565 \pm 0.010 eV$
excitation energy E_b	$2.523 \pm 0.014 eV$	$2.561 \pm 0.010 eV$
excitonic coupling V_{exc}	$0.25 \pm 0.017 eV$	$-0.064 \pm 0.008 eV$
center-center distance R_{ab}	$4.25 \pm 0.08 \text{Å}$	$8.33 \pm 0.24 \text{Å}$
angle between long axes	$6.0 \pm 1.7^\circ$	$34.0 \pm 4.0^\circ$
angle between short axes	$174.0 \pm 2.6^\circ$	$122.0 \pm 3.9^\circ$
distance of charge centers R_{cc}	5.42Å	7.57Å

V. FIGURE CAPTIONS:

Figure 1:

The atom numbering for PIC is shown as it is used to tabulate the parameters

Figure 2:

The experimental absorption spectrum⁴ of monomeric PIC (dots) is compared with a calculated spectrum (full line) from the displaced oscillator model. The calculated spectrum was shifted to reproduce the absorption maximum at 19100cm^{-1}

Figure 3:

Starting from a sandwich (a) or brickwork (b) structure relative stable dimer configurations evolved. The figure shows representative snapshots.

Figure 1:

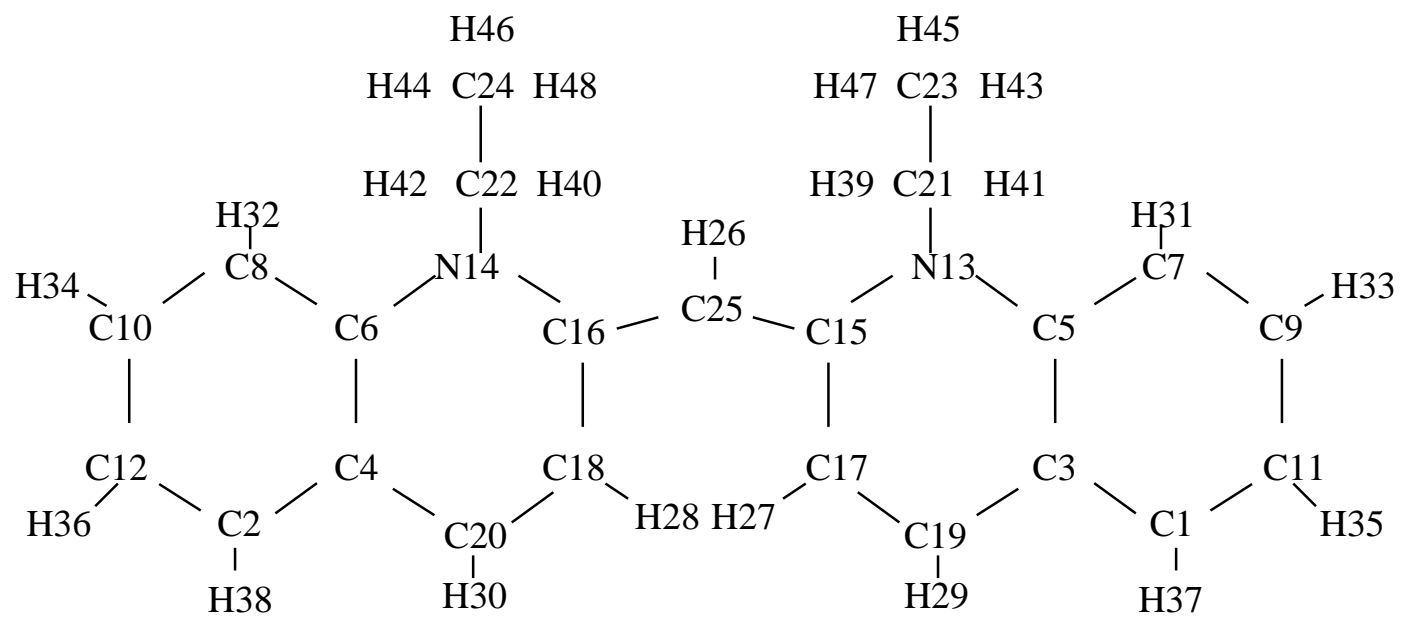


Figure 2:

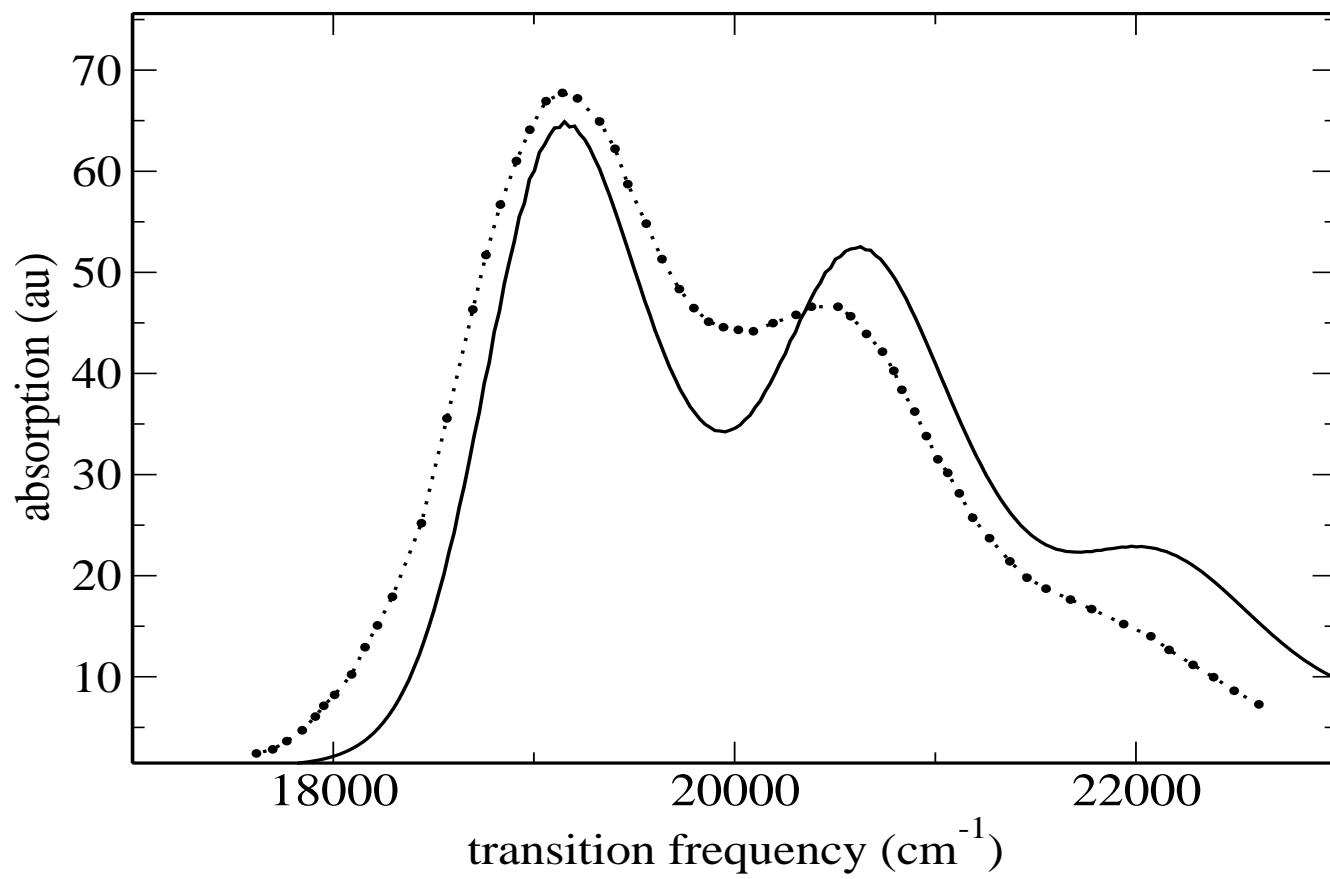


Figure 3:

